EVOLUTION OF GALAXY CLUSTERING IN THE HDF FIELDS

S. ARNOUTS
ESO- European Southern Observatory, Karl-Schwarzschild-Str. 2,
D-85748 Garching bei München, Germany

We present an analysis of the redshift evolution of the galaxy clustering in HDF-North and South . Our results show that in both fields, a similar behaviour of the galaxy clustering is observed. The HDF population appears to be anti-biased ($b \leq 1$) at $z \leq 1.5$ and the bias increases at higher redshift up to $b \simeq 2$ at $z \sim 3$. This supports the picture that high-z galaxies are biased tracers of the dark matter with a bias b strongly increasing with redshift. Finally we estimate the cosmic error budget and show that in the case of the HDF fields, the nearly Poissonian errors are dominant.

1 Introduction

In the local universe, large spectroscopic surveys have shown that the correlation length depends on morphological type and/or absolute magnitude: more luminous and/or early-type galaxies appear to have higher clustering than faint and/or late-type galaxies. However, these local observations can be reasonably well reproduced by a large variety of sensible cosmological models, while differences are expected at higher redshifts. At increasing redshift, spectroscopic surveys have found a decline of the correlation length with redshift up to $z \sim 1.5$. New insight has been reached with the discovery of a large number of galaxies at $z \simeq 3$ (Lyman-Break Galaxies, hereafter LBGs). The clustering of these primordial galaxies have been found to be at least comparable to the local value (Adelberger et al. [1]), suggesting that the LBGs are biased tracers of the underlying dark matter and formed preferentially in massive dark matter haloes.
An alternative way to probe fainter galaxy populations in a large redshift range is to apply the photometric redshift technique in extremely deep multi-colour observations like the Hubble Deep Field (HDF). Such an analysis in the HDF-North has allowed to study the redshift evolution of the clustering up to $z \sim 4.5$ for one thousand of low luminosity galaxies (Arnouts et al. [2]). Nevertheless the reliability of the results in the HDF-North can be affected by the smallness of the observed field. In particular, it is not clear to what extent a region of a few square arcminutes

can be considered representative of the properties of the whole Universe. In this context the HDF-South offers a unique opportunity to test the robustness of HDF-North results, due to their mutual independence.
In this talk, we discuss the main properties of the galaxy clustering from the two HDF fields. We present a theoretical estimate of the cosmic errors in the clustering measurements that we apply to the HDFs.

2 Redshift evolution of the galaxy clustering

We have applied the photometric redshift technique to the HDF fields to get the redshift of galaxies between $0 \leq z \leq 4.5$, as described in Arnouts et al. [2], [3]. Then in different redshift intervalles we have computed the angular correlation function (ACF) using the estimator of Landy & Szalay [6]. Since photometric redshifts are affected by large redshift uncertainties with typical rms of $\sigma(z) \sim 0.1 - 0.2$ at $z \leq 1$ and $z \geq 1.5$ respectively as well as catastrophic events, this could affect the ACF measurements. From our analysis in the HDF-North, we have used Monte-Carlo simulations to obtain statistical errors in each redshift intervalle and define an upper-limit to the amplitude of the ACF assuming that the contamination effects are due to uncorrelated population. In the HDF-South, we have taken the non gaussianity of the redshift uncertainties into account directly in the ACF measurement by weighting each galaxy according to its redshift probability distribution function (see Arnouts et al. [3] for details).
The behaviour of the amplitude ($A_\omega(10'')$) with redshift for the HDF fields is shown in Figure 1(left). As can be seen, in spite of the smallness of the HDF fields, the amplitudes measured in the two fields are in good agreement, showing a small field-to-field variation. The result in the HDF-South confirm the behaviour of the clustering with the redshift found in the HDF-North. Namely, the clustering amplitude declines from $z = 0$ to $z \sim 1$ and increases at higher redshifts to become, at $z \geq 2$, comparable to or higher than that observed at $z \simeq 0.25$. At $z \simeq 4$ the clustering signal measured in HDF-South is very noisy and we cannot confirm the high value of A_ω found in the northern field. Note that the weighted ACF method gives comparable results than the classical one except in the extrem redshift bins ($z \leq 0.5$ and $z \geq 3.5$) where higher values are obtained. In these bins the number of catastrophic redshifts is expected to be higher. The apparent evolution of A_ω with redshift seems to reflect the dependance of the clustering with the intrinsic luminosity of the galaxies. In Figure 1(right), we show the absolute luminosity (I_{ABS}) of the HDF population. At $z \leq 1$, the HDF population is dominated by galaxies with sub $L_\star$ luminosity $L_\star/100 \leq L \leq L_\star$ which corresponds at least to a factor 1-100 fainter than the population of the APM (Loveday et al. [7]). At $z \geq 1.5$, the luminosity of HDF population is $L_\star/10 \leq L \leq 5L_\star$ which is also a factor $\sim$10 fainter than the Lyman Break Galaxies (LBGs) selected by Adelberger et al. [1].
In Figure 2(left), we show the comoving correlation length $r_0(z)$ for ΛCDM cosmology. Again we find almost constant behaviour up to $z \simeq 1$ followed by an increase up to $z \simeq 3$. Since the clustering amplitude of the dark matter decreases continuously with redshift (dashed line in Figure 2(left)), the observed increase of the galaxy clustering with redshift implies that high-z galaxies are biased tracers of the underlying dark matter. This effect is illustrated in Figure 2(right), where we show the bias parameter b as a function of redshift for the HDF fields. The observed bias for the HDF-South are in good agreement with our previous results for the northern field. In particular we observe some anti-bias ($b(z < 1) \sim 0.5$) at low redshift, while we confirm that the high-z galaxies are strongly biased with respect to the dark matter: $b(z \sim 3) \sim 2$ for the ΛCDM model. This supports a model of biased galaxy formation where b is evolving with redshift. For comparison, in the same plot we also show the theoretical expectations for the effective bias (see Moscardini et al. [8], Arnouts et al. [2] for a definition) computed using different minimum mass for the dark matter haloes ($M_{\rm min} = 10^{10}, 10^{11}, 10^{12}, 10^{13} h^{-1} M_\odot$). For

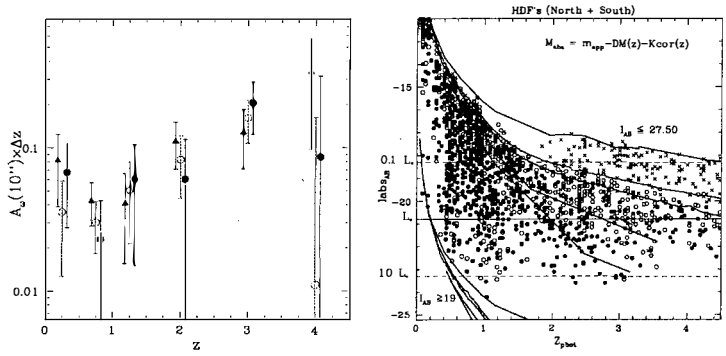

Figure 1: Left: Redshift evolution of $A_\omega \times \Delta z$ (at 10 arcsec) measured in the HDF-North (open triangles) and in the HDF-South (filled circles: standard ACF; open circles: weighted ACF); Right: Absolute magnitude (I_{ABS}) versus z for the HDF's population and compared to local L_* value.

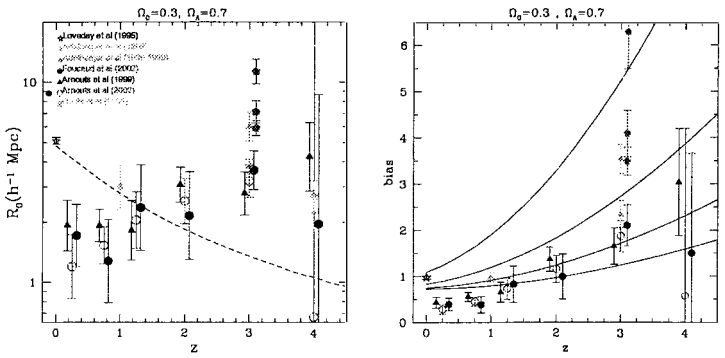

Figure 2: left: Comoving correlation length $r_0(z)$ (in ΛCDM) for the HDF populations and other surveys. The dashed line shows the prediction for the underlying dark matter; right: Bias $b(z)$. The lines represent the theoretical bias for different minimum masses: $M_{min} = 10^{10-11-12-13} h^{-1} M_\odot$ from bottom to top respectively

the ΛCDM model $M_{\rm min} < 10^{10} h^{-1} M_\odot$ is required at $z \leq 1$, $10^{10} \leq M_{\rm min} \leq 10^{11} h^{-1} M_\odot$ for $1 \leq z \leq 2$ and $M_{\rm min} \geq 10^{11} h^{-1} M_\odot$ at $< z >= 3$ are required. At redshift $z \simeq 3$, we find that the bias measured for the HDF-population ($b(z = 3) \approx 2$, for ΛCDM model) is smaller than the one observed for the bright LBGs of Adelberger et al. [1] and Foucaud [5]. These differences can be explained by the different surface galaxy densities (larger in the HDF fields, which have approximately 30 objects per square arcmin). In fact in the hierarchical galaxy formation scenario, more massive and rare objects form in rarer and higher peaks of the underlying matter density field; as a consequence they are expected to have a higher value of the bias parameter.

3 The cosmic errors

Originally, Landy and Szalay [6] have derived the variance of their estimator by assuming the weak correlation limit. The computation has been generalised by Bernstein [4] for any clustering regime taking into account higher-order correlation. The cosmic error can be split in three terms: the first (E_1) corresponds to the cosmic variance; the second (E_2) and third (E_3) terms reflect the discrete nature of the catalogue where E_2 appears only in correlated sets of points

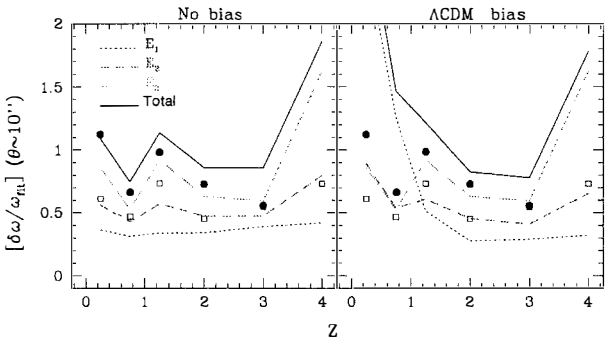

Figure 3: Comparison of the nearly Poissonian errorbars estimated for the HDF-South (filled circles) and HDF-North (open squares) with the cosmic errors (total: solid lines; E_1: dotted lines; E_2: short-dashed lines; E_3: long-dashed lines). The left and right panels refer to the no bias and ΛCDM bias models, respectively.

and E_3 contains the pure Poisson noise. The calculation of the cosmic error requires prior knowledge of statistics up to order four and its behaviours with redshift which vary with the bias parameter. A detailed discussion about how these parameters have been estimated can be found in Arnouts et al.[3]. Figure 3 shows the dependence on redshift of the errors at a fixed angular scale, $\theta = 10''$ for various bias models: no bias (left panel) and ΛCDM bias model (right panel). The theoretical expression is compared to the nearly poisson errors obtained in the HDF-South (filled circles) and the HDF-North (open squares). The nearly Poissonian errors used for the ACF measurements match quite well with E_3. In most cases, E_3 dominates the total error except at low z. Because the sample is quite sparse, we have $E_3 \geq E_2$, but E_2 is not negligible. For the bias models (right panels), the total cosmic error (solid line) has its largest values at low and high redshifts: in the first case because of the cosmic variance, in the second case because of the Poisson noise. The results show that the total cosmic error is at most $\sim$ twice larger than the poisson error and shows the same global shape. Given the level of approximation used in these works, it is thus fair to conclude that the weak clustering approximation is good enough, which confirms *a posteriori* the validity of our approach (Arnouts et al.[2,3]) to compute the errors.

Acknowledgments

I wish to thank all the people involved in the present work : S. Colombi, S. Cristiani, A. Fontana, E. Giallongo, S. Mataresse, L. Moscardini, P. Saracco, E. Vanzella.

References

1. Adelberger K.L., Steidel C.C., Giavalisco M. et al., *ApJ* 505, 18 (1998).
2. Arnouts S., Cristiani S., Moscardini L. et al., *MNRAS* 310, 540 (1999).
3. Arnouts S., Moscardini L., Vanzella E. et al., *MNRAS* 329, 355 (2002).
4. Bernstein G.M., *ApJ* 424, 569 (1994).
5. Foucaud S., in this proceeding
6. Landy S.D. and Szalay A.S., *ApJ* 412, 64 (1993)
7. Loveday J., Maddox S.J., Efstathiou G., Peterson B.A., *ApJ* 442, 457 (1995)
8. Moscardini L., Coles P., Lucchin F., Matarrese S., *MNRAS* 299, 95 (1998)